Journal of Japan Association for Earthquake Engineering, Vol.15, No.3, 2015

LONG-TERM MONITORING OF AMPLITUDE DEPENDENT DYNAMIC CHARACTERISTICS OF A DAMAGED BUILDING DURING THE 2011 TOHOKU EARTHQUAKE

Masato MOTOSAKA[1], Tsoggerel TSAMBA[2], Kazushi YOSHIDA[3], and Kazuya MITSUJI [4]

[1] Member, International Research Institute of Disaster Science, Tohoku University, Prof. Dr. Eng.
e-mail: motosaka@irides.tohoku.ac.jp
[2] Student Member, Graduate School of Engineering, Tohoku University, Graduate Student (Currently, RCAG, Mongolian Academy of Sciences)
e-mail: tsoggerelt@gmail.com
[3] Graduate School of Engineering, Tohoku University, Graduate Student (Currently Sendai City)
e-mail: k-yoshida@hjogi.pln.archi.tohoku.ac.jp
[4] Member, Faculty of Education, Art and Science, Yamagata University, Assoc. Prof. Dr. Eng.
e-mail: mitu@e.yamagata-u.ac.jp

ABSTRACT: This paper describes the amplitude-dependent dynamic characteristics of a nine-story building in Sendai before, during, and after the 2011 Tohoku earthquake. The dynamic hysteresis characteristics are investigated using actual observations. Findings on induced higher harmonics on the basis of wavelet analysis suggest partial uplifting in the transverse direction. These features are consistent with the damage. Using long-term monitoring data from micro to strong motions in the building (40 years since its completion), the historical changes in the dynamic characteristics are also explored.

Key Words: 2011 Tohoku Earthquake, Amplitude Dependent Dynamic Characteristics, Partial Uplifting, Damaged Building, Long-term Monitoring

1. INTRODUCTION

The Great East Japan Earthquake (Mw 9.0), which occurred on March 11, 2011, hereafter denoted as the 2011 Tohoku Earthquake, inflicted severe damage in wide area of Eastern Japan, particularly the Tohoku region. The long period of continuous strong motion caused vibrational damage to several buildings.

Seismically retrofitted eight- and nine-story buildings at Tohoku University’s Aobayama Campus in Sendai suffered severe damage. Despite the earthquake-inflicted damage and the subsequent dismantling and repairs, very valuable observation records were obtained with maximum acceleration of 333 cm/s/s on the first floor and 908 cm/s/s on the ninth floor in the building of departments of Civil Engineering and Architecture, School of Engineering, Tohoku University. The building is hereafter denoted as 'THU building'. The authors have analyzed the amplification characteristics of the observed records at Aobayama in relation to the records from beneath the Sumitomo Building near Sendai Station, which belongs to the Sendai seismic network. The data suggests that Aobayama Hill experienced two-times amplification around the one-second period contents compared to Sendai Station, and that the amplification characteristics were the same as those recognized in the 1978 Miyagi-ken Oki earthquake. The authors have indicated that one of the major factors contributing to the damage to the nine-story building was resonance, owing to the ground motion with the one-second period contents.

Based on investigation on the observed ground motions and building damage, the authors have reported overview of the ground motions characteristics and building damage[1)], and have reported the azimuth dependent ground motion amplification characteristics on Aobayama Hill[2)]. Despite the previous analytical record of the observations for THU building[3)], the directional differences in the building's dynamic behaviors are still not sufficiently investigated.

In this study, however, the authors describe the amplitude-dependent dynamic characteristics of the building from micro tremors to the strong-motion level based on long-term monitoring data for about 40 years, since the completion of the building, which was damaged by the 2011 Tohoku Earthquake. The monitoring data include the main shock from the Tohoku Earthquake, a foreshock, and aftershocks. The authors also describe the differences of dynamic hysteresis characteristics in horizontal two directions and changes in the dynamic characteristics that resulted from temporal reinforcement work in areas affected by the 2011 Tohoku Earthquake.

Prior studies on the dynamic characteristics of buildings include the papers by authors[4)], and Kashima[5)] for a soil-structure system of an eight-story SRC building from 1998–2005, and Kawashima et al.[6)] for the same building from 2005‐2008. Kashima also reported changes in the dynamic characteristics of the same building for the 2011 Tohoku Earthquake[7)]. Moreover, Ogata et al.[8)] reported the changes of the dynamic characteristics of a nuclear reactor building. However, the investigation of nonlinear dynamic behavior based on observation data, such as nonlinear dynamic hysteresis or partial uplifting is not sufficiently performed.

2. OBJECTIVE BUILDING AND ITS DAMAGE

2.1 Objective Building

The objective building is THU building, which is a nine-story non-full web type SRC building, completed in 1969. The first two floors form its lower portion with set back at the 3rd floor (refer to the overview of the building in Photo 1). Fig. 1 shows the floor plan of the first and third floors. Seismic resistant elements comprise the columns, the shear walls of the gable sides, and the core walls around the staircases. The building is nearly symmetrical in the north–south (transverse: TR) direction with uniaxial eccentricity in the east–west (longitudinal: LN) direction. Fig. 2 shows the topography of the building's surroundings and cross-sections of the ground. Fig. 3 shows the two soil profiles of the site. The building is supported by a 12-m long RC cross-pile with an N-value of 50 for the tip of the pile at the building's west side and 30 for the east side. The building experienced the 1978 Miyagi-ken Oki earthquake. Shiga et al.[9)] provided a detailed report of the damage due to this earthquake. From fall 2000 to spring 2001, seismic retrofitting was performed. Fig. 4 provides a breakdown of the seismic retrofitting. This involved replacing the damaged gable shear walls (R1), increasing the number of braces to prevent torsional motion (R2), reinforcing the boundary beams near the core walls (R3), and reinforcing the floor to transfer the seismic load on the building to both gable walls (R4). R1 seismic retrofitting was performed on all floors, R2 on floors 3–8, R3 on all floors, and R4 on floors 3–9. The seismic index of the building (Is) before and after the seismic retrofitting work is listed in Tables 1 and 2, respectively. The Is value increased from 0.54 to 0.84 at the heavily damaged third floor in the transverse direction

The authors performed vibration tests using an exciter before and after the seismic retrofitting, and confirmed the changes of dynamic characteristics along with estimating the stiffness reduction owing to the damage due to the 1978 Miyagi-ken Oki earthquake[4)]. Furthermore, the authors evaluated the sway and rocking ratios before and after the earthquake (ref. to Appendix). After seismic retrofitting, the building experienced the M7.2 Miyagi-ken Oki earthquake on August 16, 2005 and the M7.2 Iwate-Miyagi Nairiku Earthquake on June 14, 2008.

The authors investigated the amplitude-dependent dynamic characteristics based on strong motion and microtremor observations for 40 years after the construction of the building[4)10)]. In addition, the authors have performed continuous observations since December 2007 by placing high-sensitive MEMS sensors with broad dynamic ranges on the 1st, 5th, and 9th floors of the building. This system allowed the observation from microtremors to strong motions. The authors are working toward system development by combining structural health monitoring with an earthquake early warning system [11)].

Photo 1　Overview of the building

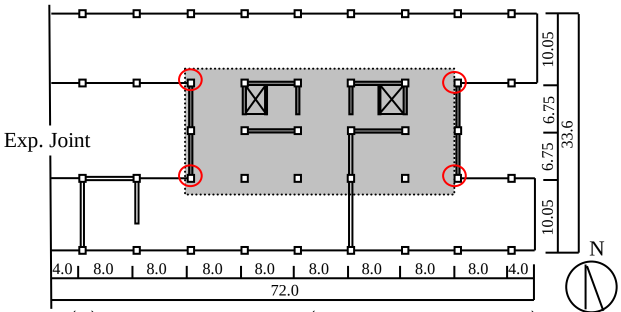

(a) 1st floor plan　(unit of length: m)

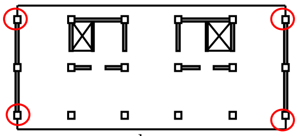

○: Damaged pillars
(3rd floor pillar legs)

(b) 3rd floor plan

Fig. 1 Plan of the objective building

Objective Building

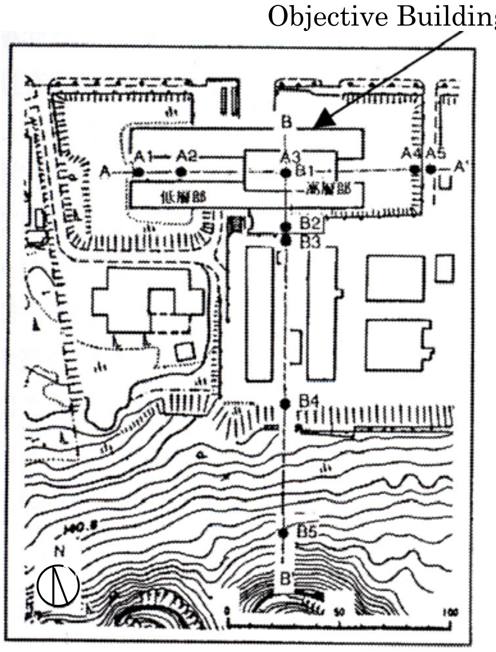

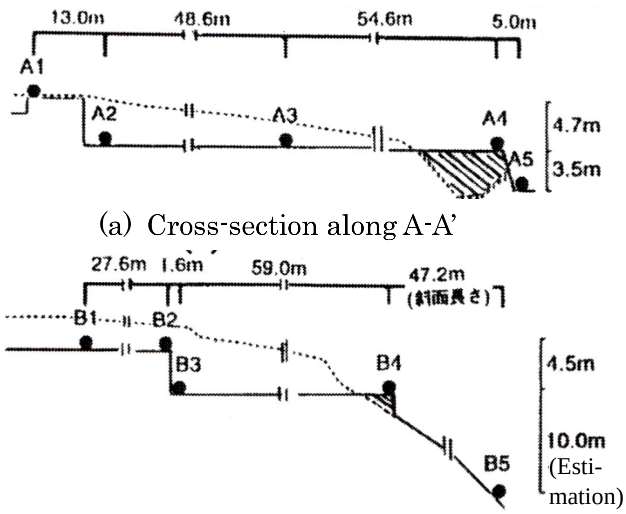

(a) Cross-section along A-A'

(b) Cross-section along B-B'

Fig. 2 Building topographic map and foundation cross-sections

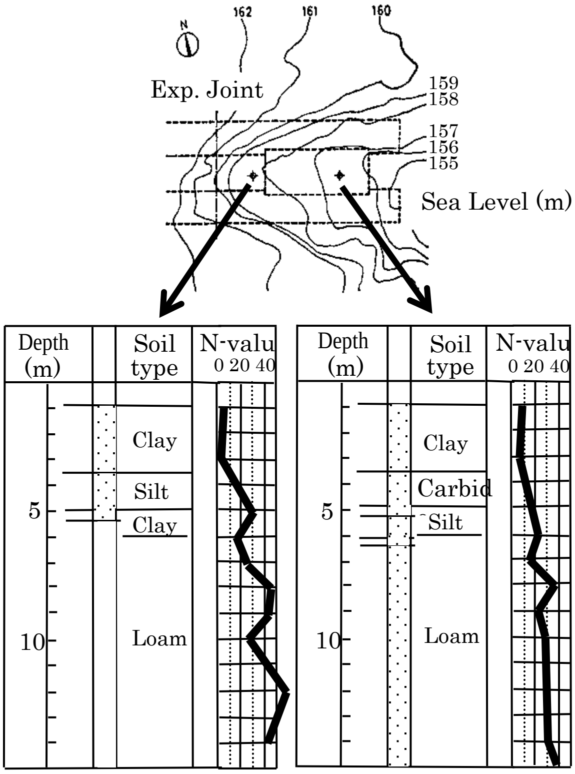

Fig. 3 Soil profiles of the site

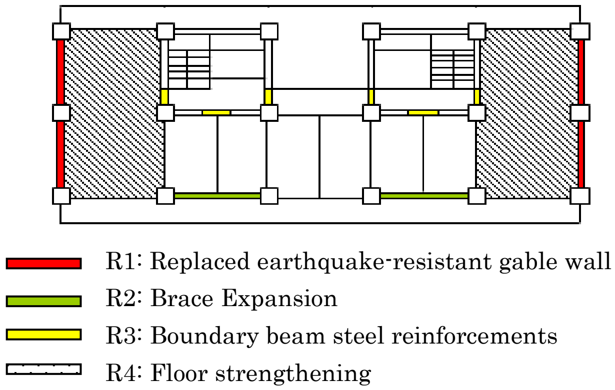

Fig. 4 Overview of seismic retrofit

Table 1 Is-values before the seismic retrofit

Floor	1	2	3	4	5	6	7	8	9
TR	0.56	0.61	0.54	0.57	0.68	0.69	0.72	0.79	1.04
LN	0.55	0.94	0.91	0.55	0.56	0.57	0.63	0.74	0.76

Table 2 Is-Values after the seismic retrofit

Floor	1	2	3	4	5	6	7	8	9
TR	0.75	0.88	0.84	1.01	1.02	1.05	1.13	1.33	1.32
LN	0.63	1.12	1.45	0.88	0.84	0.93	1.02	1.20	1.07

2.2 Summary of the damage from the 2011 Tohoku Earthquake

The authors observed significant damage to all the base of the four corners columns on the 3rd floor during a survey conducted the day after the 2011 Tohoku Earthquake. Photos 2–4 show the damage to the building. The base of the columns was heavily damaged because of the varying axial forces due to the bending vibration of the east–west gable shear walls (multi-story shear walls). Buckling of the steel web and fracturing and buckling of the main bars was also observed. In addition, from the cracks in the gable walls in the 3rd floor (Photo 4), the authors considered the possibility of partial uplifting of the upper part from the 3rd floor after the column base's failure, and analyzed the observed waveform focusing on the induced higher harmonic frequency contents[12)]. After the April 7 aftershock, the authors confirmed the peeling of the cover concrete of middle column on the east side and buckling of the main bar; although, in the survey taken the day after the main shock on March 11 the authors did not observe peeling of the cover concrete of the middle column.

Photo 2 Damaged building viewed from the east side

Photo 3 Heavily damaged southeast corner column base

Photo 4 Crack in the 3rd floor shear wall

The authors inspected the condition of the exposed main bars of the heavily damaged columns' base a day after the main shock of Tohoku Earthquake, and confirmed the existence of rust in the failure sections due to past earthquake and also new failure due to the Tohoku Earthquake.

3. ANALYSIS OF THE OBSERVED RECORD DURING THE TOHOKU EARTHQUAKE

3.1 Sensor locations and observation records

The SMAC-MD-type strong-motion seismometers (Building Research Institute management) are installed on the 1st and 9th floors of the building. Since December 2007, the authors have also installed a monitoring system in the Tohoku University Disaster Control Research Center that makes possible continuous observations of movements ranging from microtremors to strong motion. This system uses three seismometers with three-component high-sensitive MEMS sensors (microSMA) on the 1st, 5th, and 9th floors. Fig. 5 shows the location of the sensors.

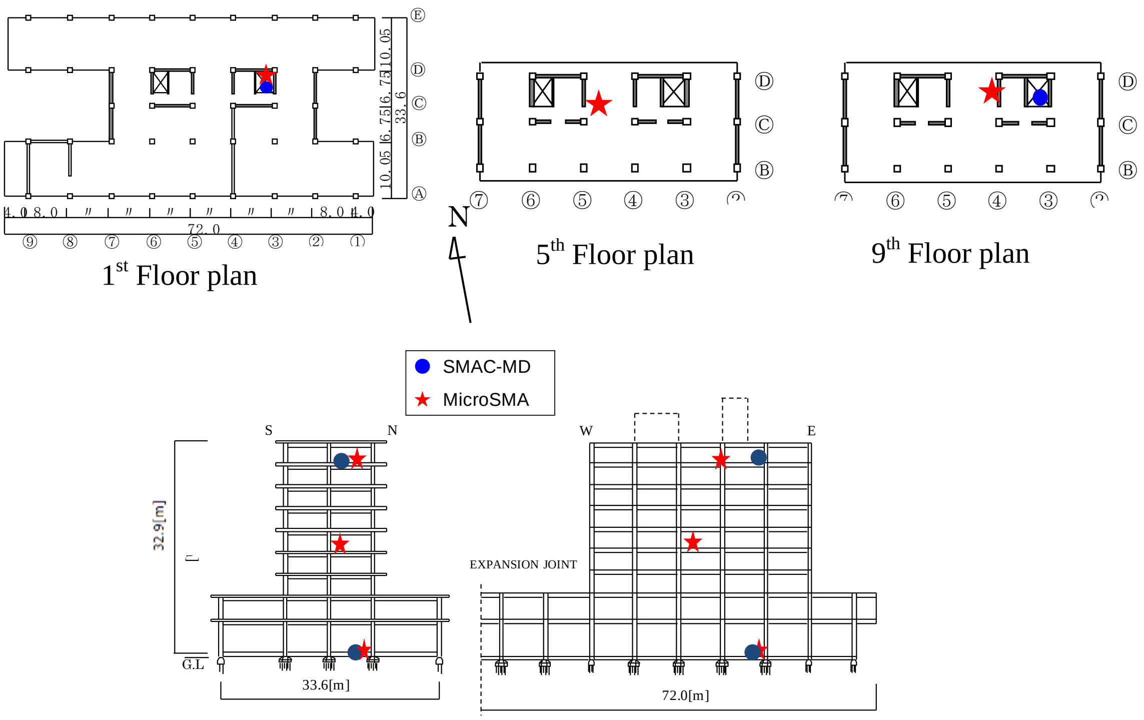

Fig. 5 Configuration of THU Building and Sensor locations

Fig. 6 shows the two horizontal and vertical waveforms during the 2011 Tohoku Earthquake on the 1st and 9th floors. Fig. 7 compares the strong-motion records during the 2011 earthquake and the 1978 Miyagi-ken Oki Earthquake at the same location for the north–south directional component (transverse direction). Fig. 8 shows the pseudo-velocity response spectra for these records (5% decay). The observation records during the Tohoku Earthquake are analyzed by dividing two phases, Phase A and Phase B (ref. to Fig. 6).

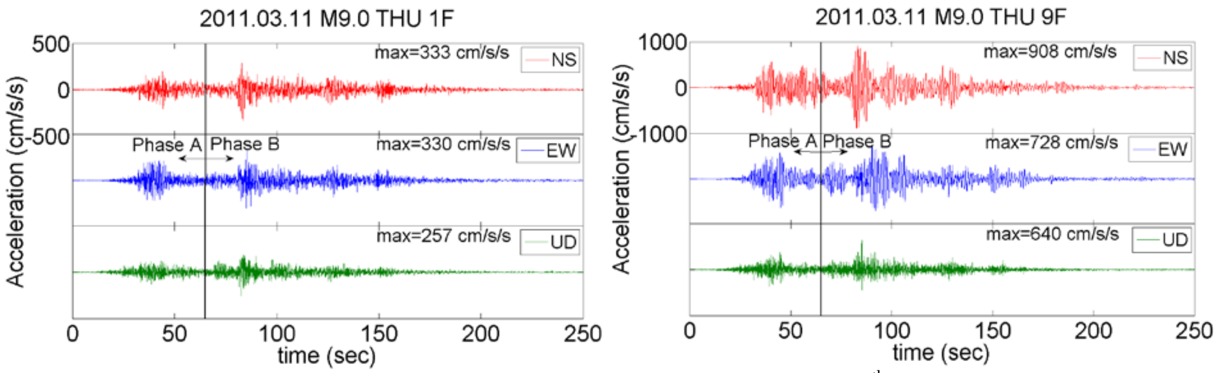

(a) 1st Floor record (b) 9th Floor record

Fig. 6 Strong-motion records for the 2011 Tohoku Earthquake at THU building

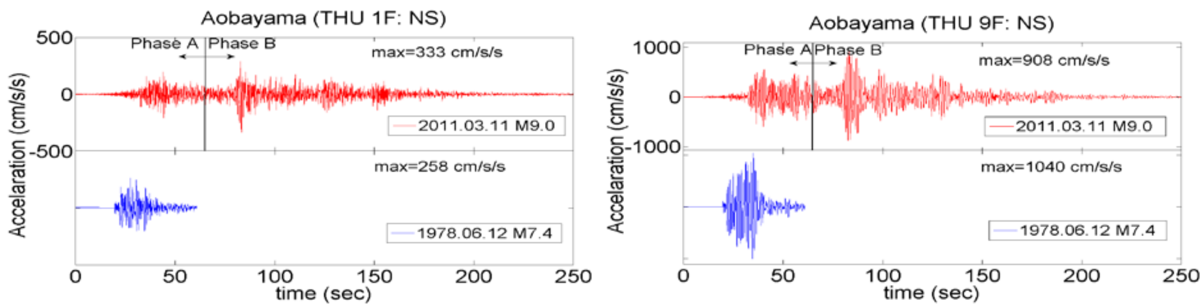

(a) 1st Floor record (b) 9th Floor record

Fig. 7 Comparison of the records for the 2011 Tohoku Earthquake and the 1978 Miyagi-ken Oki Earthquake (north–south direction)

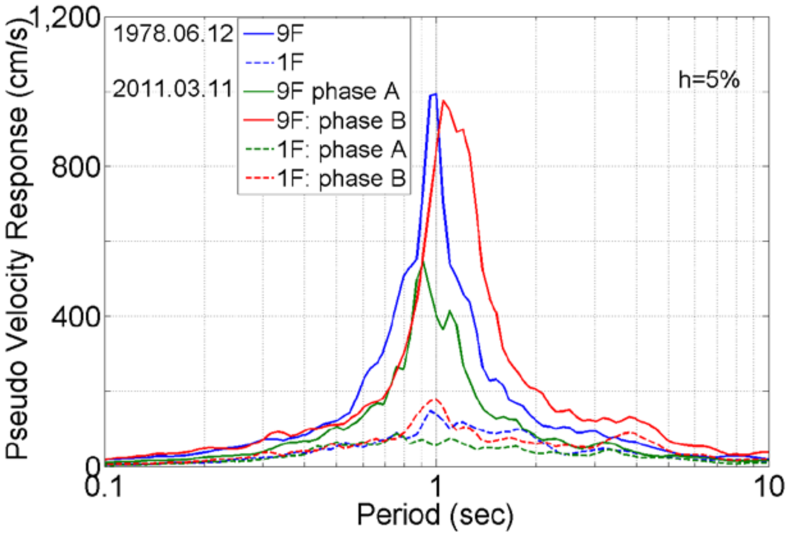

Fig. 8 Comparison of the pseudo-velocity response spectra for the 2011 Tohoku Earthquake and the 1978 Miyagi-ken Oki Earthquake (north-south direction)

By the way, the authors analyzed the ground motion amplification characteristics of the Aobayama to Sumitomo Building near Sendai Station, reported that the amplification characteristics in the north–south direction showed no amplification for Phase A at around 1s period contents, whereas Phase B showed two times amplification similar to the 1978 Miyagi-ken Oki Earthquake[2)]. It is noted that the resonance of the building to the amplified shaking is one of major factors contributed to the damage.

3.2 Dynamic hysteresis characteristics

To analyze the dynamic hysteresis characteristics from the actual records, the authors calculated the relative displacement from the displacement waveforms obtained by the double integration of the acceleration waveforms for the 1st and 9th floors. Fig. 9 shows the relative displacement waveform for the north–south direction (transverse direction). The maximum relative displacement is 31 cm. It is possible to evaluate the apparent dynamic hysteresis characteristics, assuming that the relative displacement waveform apparently represents deflection of the building and the 9th floor acceleration record corresponds proportionally to the inertia force acting on the building. Fig. 10 shows the dynamic hysteresis characteristics in the north–south direction for several time sections.

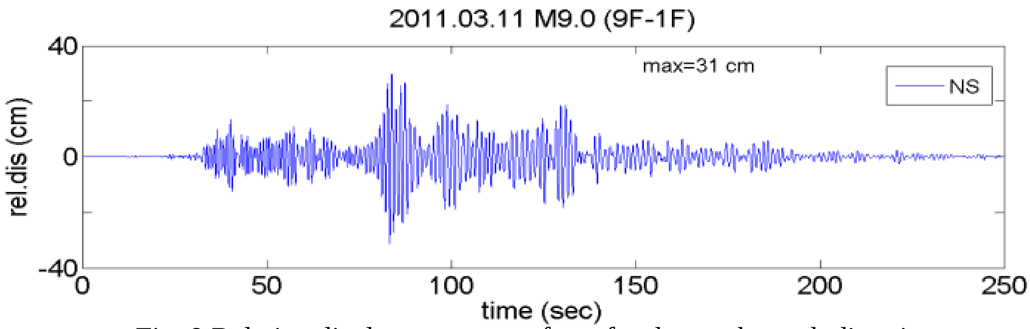

Fig. 9 Relative displacement waveform for the north-south direction

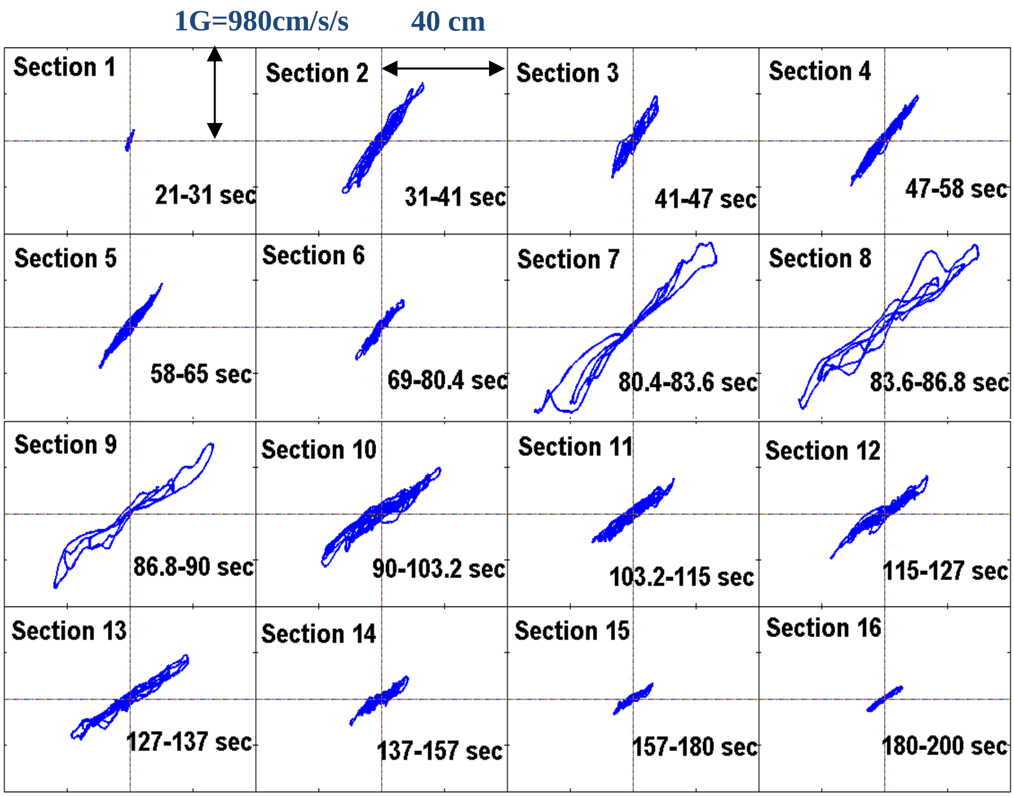

Fig. 10 Dynamic hysteresis characteristics in the north-south direction for various times

The findings from this figure are as follows:

1) Starting from linear behavior at smaller amplitude level, hysteresis shows the reverse 'S' shape slightly as recognized in section 5. Then shows linear behavior but the stiffness is reduced in section 6 compared to section 1.
2) Then, with increasing displacement, the hysteresis shows softening and hysteretic loop is recognized only for the larger displacement level. The hysteresis shows the origin oriented behavior as recognized in (section 7).
3) The fundamental natural frequency decreases from 1 Hz to 0.8Hz from section 7 to section 10. This natural frequency change corresponds to the apparent stiffness reducing to 64%.
4) Then decreasing the displacement, the hysteresis shows the characteristic reverse 'S' shape in section 9. Although the amplitude decreases from Section 9 to Section 10, stiffnesses are almost the same, which consistent with the dominant frequency reduction.
5) Then decreasing displacement gradually returns to linear behavior with the reduced stiffness in sections from 13 to 16 compared to section 6. The stiffness change is consistent with microtremor observation before and after the earthquake.

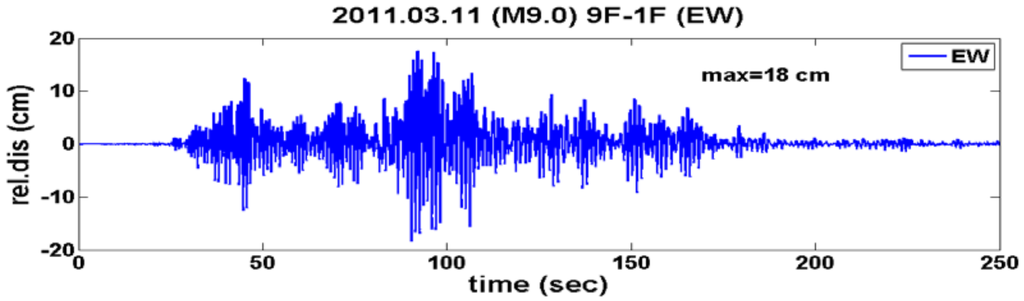

Fig. 11 Relative displacement waveforms in the east-west direction

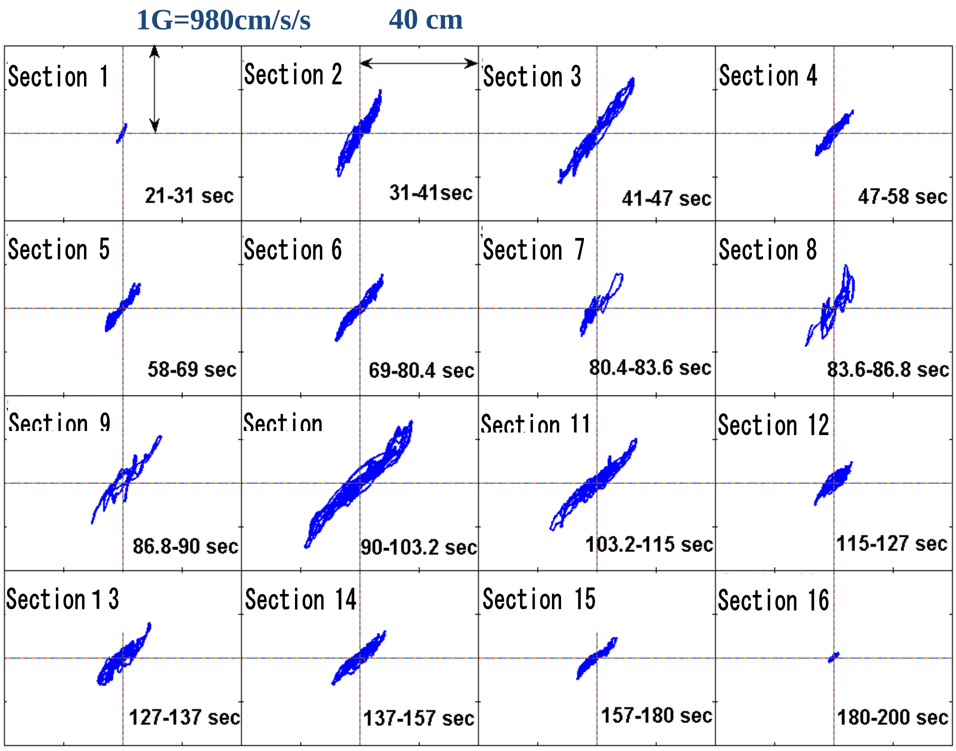

Fig. 12 Dynamic hysteresis characteristics in the east-west direction for different times

Fig. 11 shows the relative displacement waveform for the east–west (longitudinal) direction. Moreover, Fig. 12 shows the dynamic hysteresis characteristics in the east–west direction for the exact same time sections in Fig. 10. The following findings are inferred by comparing Figs. 11 and 12 with Figs. 9 and 10 where the direction is different.

1) The relative displacement in the east–west direction is 18 cm, which is 58% of 31 cm in the north–south direction.
2) The time when the largest value for relative displacement occurred was approximately 82 s (section 7) in the north–south direction and 90 s (section 10) in the east–west direction.
3) Looking at the dynamic hysteresis characteristics for the time near the largest value of the east–west direction (section 10), the origin oriented hysteresis cannot be observed characteristics as is recognized in the north–south direction.
4) In the east–west direction, the effect of higher modes' vibration was clearly confirmed in sections 8 and 9.

3.3 System identification

To analyze the non-stationary dynamic characteristics associated with the nonlinearity of the building structure, the authors conducted system identification using the extended Karman filter and evaluated the natural frequency and damping factor of an equivalent single degree of freedom system[13).]

Fig. 13 shows the identified natural frequency and damping factor for the north–south and east–west directions. In this figure, the estimated waveforms using parameters obtained from the system identification and the relative displacement waveforms obtained from observations are comparatively shown. The smoothed trends in the time direction for the identified natural frequency and damping factor are also shown.

The following findings are found from these figures.

1) In the north–south (transverse) direction, the natural frequency decreases to approximately 1.0 Hz for phase A, whereas for phase B it decreased to approximately 0.8 Hz. Relatively large amplitudes continues until the 135-second point. Although the amplitude after this point decreases, there is no change in natural frequency. This means that even if the amplitude is small the building vibrates by the same stiffness as the largest amplitude point.
2) The damping factor in the north–south direction increases along with the amplitude (Fig. 10, section 7). In the time section with the reverse 'S' shape, the damping factor decreases as the amplitude increases.
3) The natural frequency of the microtremor level for the day prior to the earthquake was 1.61 Hz in both directions, as explained later. Although the natural frequency in the east–west (longitudinal) direction decreases to 1.0 Hz in the phase A, which is almost the same as in the north–south direction, the natural frequency for phase B decreases to approximately 0.9 Hz and recovered to 1 Hz with decreasing amplitude.
4) The smoothed damping factor for the east–west direction is larger than the north–south direction. This is attributed to the differences in hysteretic energy consumption.

3.4 Partial uplifting

In general, when the partial uplifting of a structure occurs, the odd higher harmonic components in the horizontal direction and the even higher harmonic components in the vertical direction are indused[14)].

Fig. 14 shows the wavelet coefficients, based on the analysis using Morlet complex wavelets[15)], of the non-stationary characteristics of the acceleration waveforms for the 9th floor for section 10 (80–90 s) with large amplitude vibrations. Figs. 15(a) and 15(b) show the wavelet coefficients vertical direction acceleration waveforms for the 9^{th} and 1^{st} floor, respectively. The following findings are obtained from these figures.

1) From the wavelet coefficient of the vertical direction for the 9th floor, the 2-times higher harmonic components (1.6–1.8 Hz) are clearly recognized in sections 7–9 in Fig. 11; however, this frequency components for the vertical direction on the 1st floor cannot be seen and thus the

vertical motion at the 9th floor is considered as the induced vertical motion.

2) In addition, the 4- and 6-times higher harmonic components are induced and, in combination with the 2-times higher harmonic components, the even higher harmonic components are induced consistent with the amplitude level. This suggests partial uplifting of the upper part from the 3rd floor.

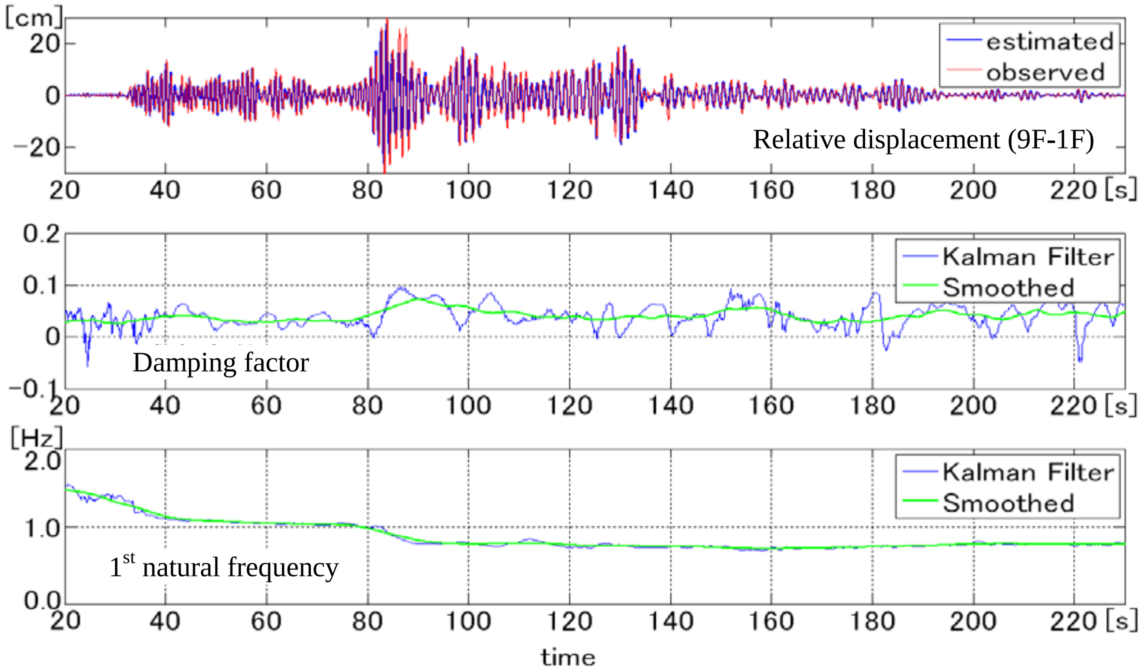

(a) North-south direction (Transverse direction)

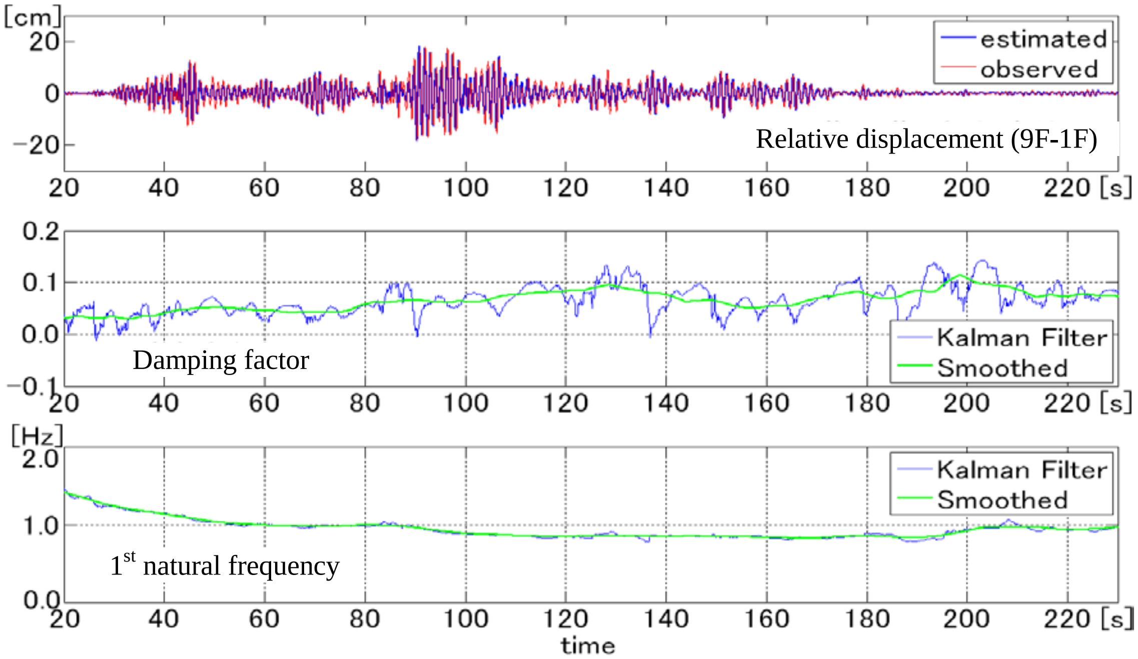

(b) East-west Direction (Longitudinal Direction)

Fig. 13 Horizontal bi-directional damping constant and natural frequency obtained from system identification

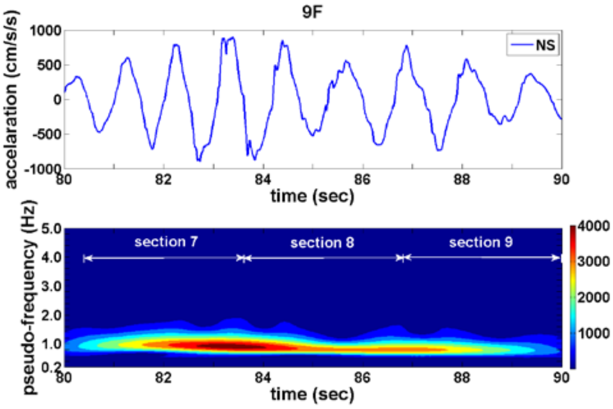

Fig. 14 Wavelet coefficients of the 9th floor north-south directional acceleration waveform

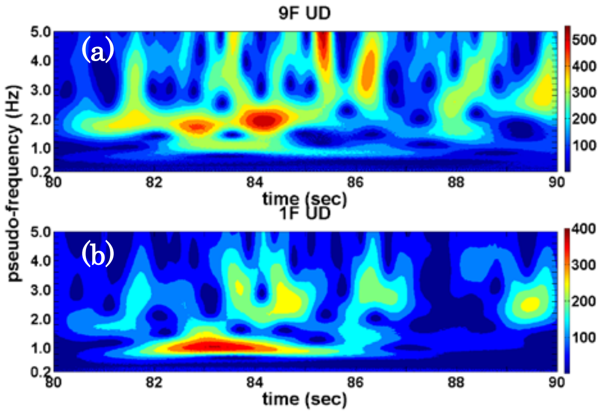

Fig. 15 Wavelet coefficients for the (a) 9th floor and (b) 1st floor vertical acceleration waveforms

4. AMPLITUDE-DEPENDENT DYNAMIC CHARACTERISTICS BASED ON LONG-TERM MONITORING

4.1 Dynamic characteristics before and after the foreshocks, main shock, and aftershocks of the 2011 Tohoku Earthquake

As noted above, the authors performed microtremor observations, forced vibration tests, and earthquake observation data analysis for the building since its completion in 1969. The authors investigated the amplitude-dependent dynamic characteristics before and after the seismic retrofitting, which took place from the fall of 2000 to spring of 2001[4)].

Table 3 lists the first natural frequencies for the foreshocks, main shock, and aftershocks of the 2011 Tohoku Earthquake and also for the microtremors before and after these earthquakes. The natural frequencies are evaluated as peak frequencies of the transfer functions obtained from the 1st and 9th floor records as natural frequencies.

The natural frequencies at the microtremor-level in both directions prior to the Sanriku Oki foreshock occurred on March 9, were 1.61 Hz, whereas the frequency at the microtremor-level after the foreshock decreased to 1.26 Hz in both directions. However, there was a relatively large decrease in the north–south natural frequency compared to the east–west direction for the main shock on March 11, which is consistent with the damage. The natural frequency decrease for Phase B was remarkable, whereas the stiffness decrease to 23% in the north–south direction and 30% in the east–west direction —when squaring the ratio of the microtremor-level natural frequency to the main shock's natural frequency. Relative to the main shock, the natural frequency at the microtremor-level after the main shock decreased to 53% in the north–south direction and to 72% in the east–west direction.

The damaged building had temporal retrofitting (countermeasures by RC Pia and steel rods for varying axial force and one-span shear wall reinforcements in the four corners) done in May, 2011 to ensure that the moving of equipment and other work could be done safely. Fig. 16 shows the changes in the microtremor-level natural frequencies corresponding to the reinforcement work. The natural frequencies in the north–south and east–west directions were 1.17 Hz and 1.37 Hz, respectively, before the temporal reinforcement work and changed to 1.37 Hz and 1.48 Hz afterwards. The natural frequency changes were recognized in the transverse (north–south) direction when the bolts of the reinforcing rods were tightened and penetrated the 3rd floor to reinforce its four corner pillars, and when the one-span shear walls were added on the 3rd floor in the longitudinal (east–west) direction. Moreover, it is worth mentioning that the microtremor-level natural frequency on May 3, before the reinforcement work, was the same as the natural frequency of the microtremor-level after the aftershock on March 19. This shows that there were no changes in the natural frequency of the microtremor level even after the aftershocks on April 7 and 11, which seems to be controversy to the damage extension as described in section 2.2. But it is suggested that the visible damaged parts do not contribute to dynamic stiffness of the building in the small amplitude level like microtremor. It is necessary to collect more data in the future to interpret this phenomenon.

Table 3 Changes in natural frequencies

Date	Event name	Natural frequency (HZ)	
		NS	EW
2011/3/9	Microtremor	1.61	1.61
2011/3/9	Foreshock (Sanriku Oki)	1.26	1.26
2011/3/11	Microtremor	1.61	1.61
2011/3/11	Main shock (Phase A)	1.05	1.05
	Main shock (Phase B)	0.78	0.88
2011/3/19	Microtremor	1.17	1.37
2011/3/19	Aftershock (Ibaraki-Ken)	0.93	1.16
2011/5/3	Microtremor	1.17	1.37
2011/5/31	Microtremor	1.37	1.48

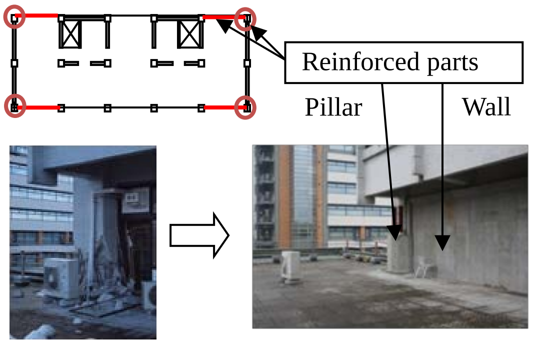

Photo 5 Temporal reinforcements to the heavily damaged 3rd floor

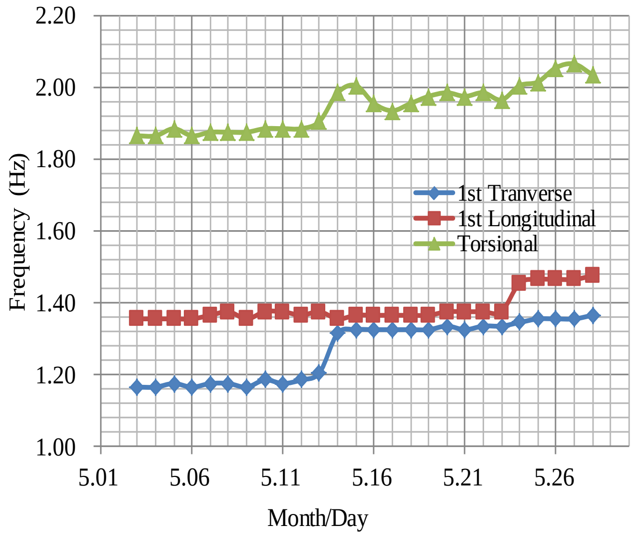

Fig. 16 Daily natural frequency changes owing to emergency reinforcement work

4.2 Amplitude-dependent dynamic characteristics based on long-term monitoring

Table 4 lists the maximum acceleration of the major earthquake observation records for approximately 40 years since the completion of the building. Similar to Motosaka et al.[4)], Fig. 17 shows the relation between the deflection angles and the 1st natural frequencies in the divided four periods as the investigation of the amplitude-dependent dynamic characteristics. In this case, the authors evaluated the deflection angles by using the maximum displacement obtained by integrating the 9th floor acceleration records, and dividing them by the building height. These four periods are as follows: term 1 is the period between the completion of the building until the 1978 Miyagi-ken Oki Earthquake; term 2 is the period from the 1978 Miyagi-ken Oki Earthquake until the seismic retrofitting in 2000; term 3 is the period between retrofitting and the 2011 Tohoku Earthquake; and term 4 is the period following the Tohoku Earthquake. Moreover, term 3 is divided into two components wherein term 3a is until the June 14, 2008 Iwate-Miyagi Nairiku Earthquake and term 3b is from June 14, 2008 until March 9, 2011. Term 4 is also divided into two parts wherein term 4a is between the 2011 Tohoku Earthquake until the time of the temporal reinforcements and term 4b is the period after the reinforcements. Fig. 18 shows the chronological change of the 1st natural frequencies from 1970 to 2011 until the temporal reinforcement works were performed. The circle marks the 1st natural frequencies obtained from the earthquake observation records, whereas the red marks earthquakes that caused damage. The blue lines show the results obtained from microtremor observation records. The figures reflect the results of the deflection angles and 1st natural frequencies shown in Fig. 17. The 1st natural frequency decreased by the damage due to the 1978 Miyagi-ken Oki Earthquake. Although then the seismic retrofitting in 2001 increased the frequency, the June 14, 2008 Miyagi-Iwate Nairiku Earthquake, that occurred after the retrofit, and the March 11, 2011 Tohoku Earthquake further contributed to the decrease.

Table 2　Maximum acceleration list of major earthquake observation records at THU building

Date	Magnitude	1 Floor　(max.acc (cm/s/s))		9 Floor　(max.acc (cm/s/s))		Area name	
		NS	EW	NS	EW		
1978/2/20	6.7	170	114	421	298	Miyagi-Ken Oki	
1978/6/12	7.4	258	203	1040	523	Miyagi-Ken Oki	
1998/9/15	5.2	138	451	190	379	Miyagi-Ken Southern	
2003/5/26	7.1			231	264	Miyagi-Ken Oki	
2003/7/26	6.2	33	27	98	102	Miyagi-Ken Northern	
2003/9/26	8.0			29	22	Tokachi Oki	
2005/8/16	7.2	87	81	329	287	Miyagi-Ken Oki	
2008/5/8	7.0	19	22	261	226	Ibaraki-ken Oki	
2008/6/14	7.2	88	70	392	293	Iwate-Miyagi inland	
2008/7/24	6.8	59	77	275	367	Iwate-Ken North Coast	
2011/3/9	7.2	37	34	171	89	Sanriku Oki	
2011/3/11	9.0	207	216	594	617	Off Pacific Coast Tohoku	(Phase A)
		333	330	908	728		(Phase B)
2011/3/19	6.1	15	18	34	56	Ibaraki-ken Northern	
2011/4/11	7.0	72	70	141	172	Fukushima-Ken Southern	
2011/4/12	6.4	24	28	43	84	Fukushima-Ken Oki	
2011/4/23	5.4	17	27	23	57	Fukushima-ken Oki	
2011/7/10	7.1	21	18	95	58	Sanriku Oki	
2011/7/23	6.5	10	11	60	42	Miyagi-Ken Oki	
2011/7/25	6.2	48	62	106	99	Ibaraki-ken Northern	
2011/7/31	6.4	36	31	70	45	Fukushima-ken Oki	

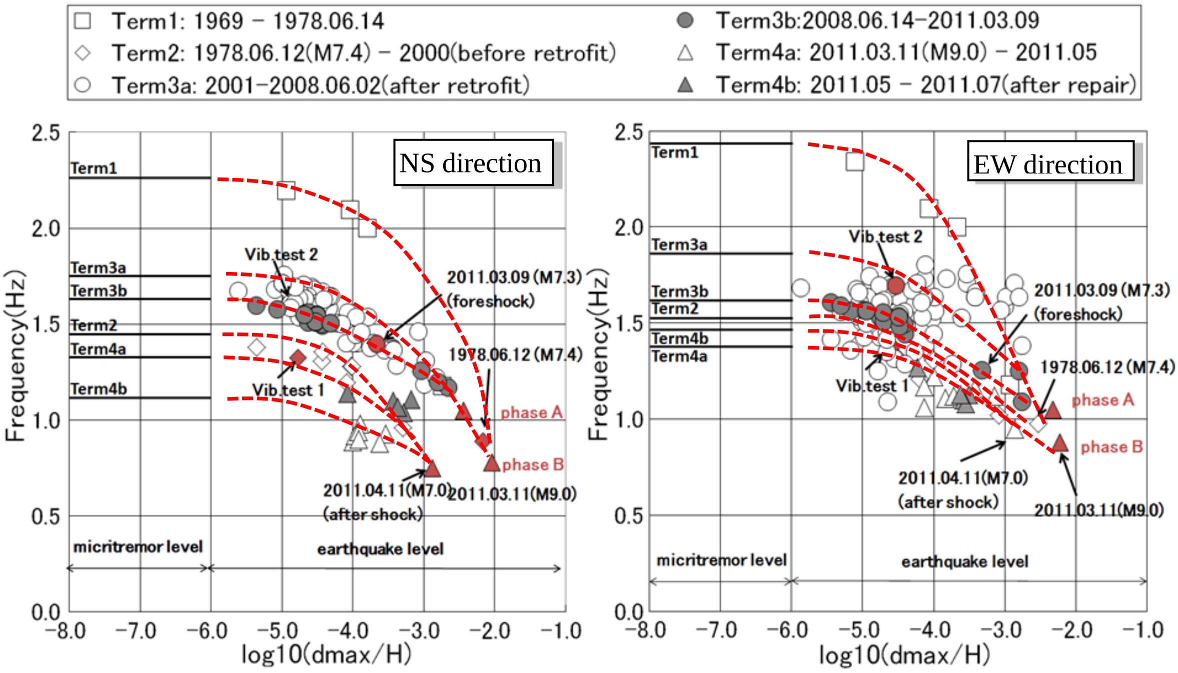

Fig. 17 Relation between deformation angle and primary natural frequency

It is found from the figures, the following findings are obtained.

1) The amplitude level of the Tohoku Earthquake for phase A is smaller in the north–south direction than the deflection due to the 1978 Miyagi-ken Oki Earthquake, and the natural frequency is higher. On the contrary, although the amplitude is lager in the east-west direction, the natural frequency is higher. This indicates that the effect of seismic retrofit on the increase of the natural

frequency is stronger compared to the decrease in the amplitude level not to cause significant damage. In phase B, the amplitude levels are higher than the 1978 Miyagi-ken Oki Earthquake in both directions.

2) Changes in the natural frequency of the 2011 Tohoku Earthquake are larger in the north–south direction than east–west direction and correspond to the damage feature.
3) Based on the continuous observation, the natural frequency of the microtremor-level is not changed if the displacement level did not exceed the largest displacement experienced in the past, as shown in Fig. 18.

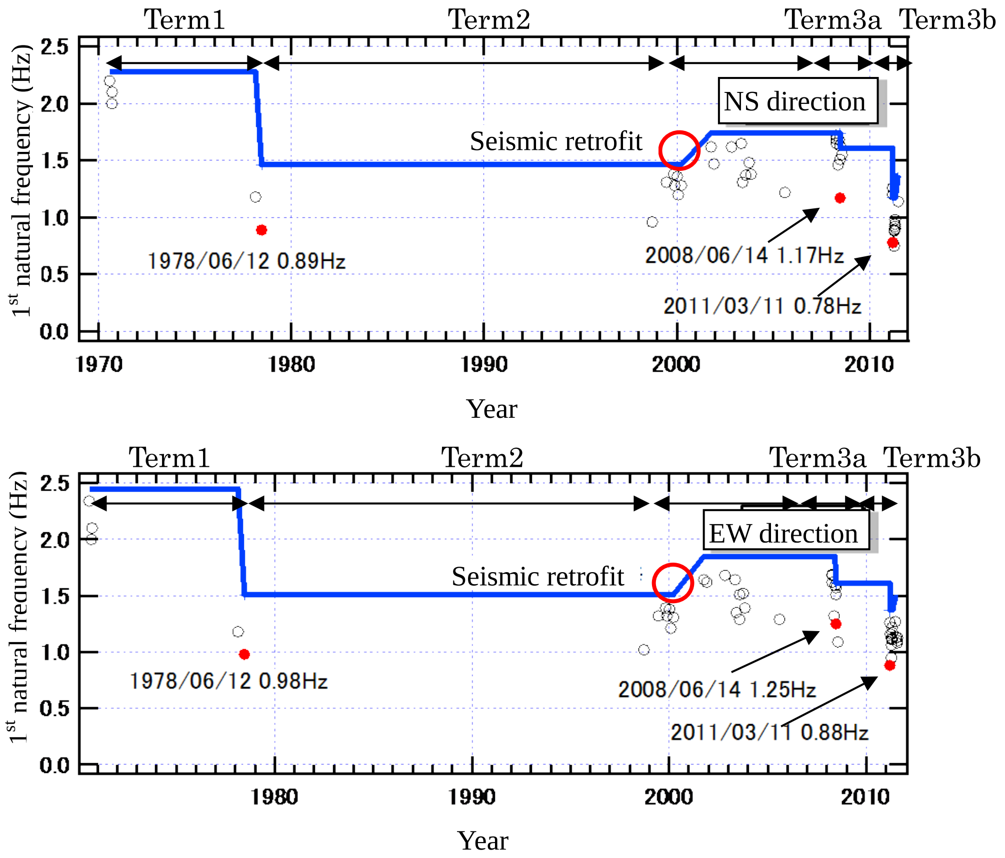

Fig. 18 Change of the 1st natural frequency (red circles denote earthquakes that caused damages)

5. CONCLUSIONS

During the 2011 Tohoku Earthquake, THU building (9-story SRC building) was heavily damaged due to resonance to the amplified one-second period contents, which was attributed to the ground conditions of the Aobayama hill. In this study, the dynamic behaviors of the building during the earthquake are investigated together with the changes of the dynamic characteristics due to the foreshock, main shock, and aftershocks. Based on the long-term monitoring (40 years) from microtremors to strong motion since the completion of the building, the amplitude-dependent dynamic characteristics are also investigated. Thus, the following findings are inferred.

1) Based on the investigation of the dynamic hysteresis for the heavily damaged north–south direction, the origin-oriented hysteresis was identified around the time of maximum deflection and the reverse ‘S’ shape hysteresis was recognized based on the actually obtained earthquake obtained records.
2) The amplitude dependency of the natural frequencies and damping factors is investigated based on the system identification using the observation data in the heavily damaged building.
3) From the nonstationary spectra based on wavelet analysis, the induced higher harmonic components were confirmed, which suggests the occurrence of the partial uplifting of the upper part of the building from 3rd floor. This is consistent with the concrete crack and main bar’s buckling of the middle column recognized

on the 3rd floor.

4) Long-term monitoring allowed compiling the amplitude-dependent dynamic characteristics of the damaged building.

The authors believe that the above information on amplitude-dependent dynamic characteristics based on long-term monitoring of the damaged building will contribute to seismic resistant design of building structures in future.

ACKNOWLEDGMENTS

The strong motion records used in this study were provided by the Building Research Institute. The authors extend our gratitude to Dr. Toshihide Kashima and other related persons who assisted the authors in this study.

APPENDIX: CHANGE OF NATURAL FREQUENCIES BASED ON VIBRATION TESTING BEFORE AND AFTER SEIMIC RETROFITTING

The authors studied the behavior of THU building that underwent seismic retrofitting from fall 2000 to spring 2001. The authors conducted forced vibration tests using an exciter before and after the retrofitting and confirmed the changes in natural frequency before and after the retrofitting. The authors also estimated the stiffness decrease owing to the building damage due to the 1978 Miyagi-ken Oki Earthquake[4]. Moreover, the sway and rocking ratios of the building were evaluated.

The appended Table 1 lists the natural frequencies before and after the retrofitting evaluated using the peak frequencies of the resonance curves. The appended Table 2 lists the sway and rocking ratios before and after the retrofitting. The data regarding the dynamic characteristics from the vibration tests will be useful for simulation analysis and for creating analytical models of the building to investigate the comparison of the dynamic behavior and damages due to the 1978 Miyagi-ken Oki and 2011 Tohoku earthquakes.

Appended Table 1 Changes in natural frequency before and after the seismic retrofitting

Direction	Mode	Vibration Test		Microtremor	
		Before Retrofitting	After Retrofitting	Before Retrofitting	After Retrofitting
EW Direction	Translational 1st	1.40 Hz	1.73 Hz	1.54 Hz	1.85 Hz
	Translational 2nd	4.40 Hz	5.00 Hz		
	Torsional 1st	2.05 Hz	2.55 Hz	2.20 Hz	2.61 Hz
NS Direction	Translational 1st	1.33 Hz	1.65 Hz	1.48 Hz	1.74 Hz
	Translational 2nd	4.40 Hz	4.80 Hz		

Appended Table 2 Sway and rocking ratios before and after the seismic retrofitting

	Direction	Observation Location	Vibration Test		Microtremor	
			Before Retrofitting	After Retrofitting	Before Retrofitting	After Retrofitting
Sway	EW Direction	Center	2.2%	4.8%	3.4%	5.2%
	NS Direction	East Side	2.9%	5.9%	3.8%	6.1%
		Center	2.4%	4.7%	3.1%	5.2%
		West Side	2.2%	4.5%	3.1%	5.3%
Rocking	EW Direction	Center	3.5%	7.7%	5.1%	8.4%
	NS Direction	Center	4.3%	9.4%	6.7%	10.6%

REFERENCES

1) Masato Motosaka: Lessons of the 2011 Great East Japan Earthquake Focused on Characteristics of Ground Motions and Building Damage, Proceeding of International Symposium on the 2011 Great East Japan Earthquake, 2012, pp.166-185.
2) Tsamba, Tsoggerel, and Masato Motosaka: SITE SPECIFIC GROUND MOTION AMPLIFICATION CHARACTERISTICS IN AOBAYAMA HILL, SENDAI, JAPAN, Proc. 9CUEE & 4ACEE, 2012, pp.291-296.
3) Motosaka, Masato, Kazuya Mitsuji, Shoko Tanaka, Toshihide Kashima, and Susumu Ohno: Change of Dynamic Characteristics of a Damaged Building Before, During , and After the 2011 Off Pacific Coast Tohoku Earthquake, Summaries of Technical Papers of 2011 AIJ Annual Meeting, Structure II, 2011, pp.45-46 (in Japanese).
4) Masato Motosaka, Yuu Yamamoto, and Takeshi Sato: Amplitude Dependent Dynamic Characteristics of an Existing Building, 13WCEE, 2004, CD-ROM No.1023.
5) Toshihide Kashima, Yoshikazu Kitagawa: Dynamic Characteristics of a Building Estimated From Strong Motion Records Using Evolution Strategy, Journal of Structural and Construction Engineering (Transaction of AIJ), Vol.77, No.602, 2006, pp.145-152 (in Japanese with English abstract).
6) Manabu Kawashima, Masayuki Nagano, Toshihide Kashima, and Michio Iguchi: Varying of dynamic characteristics of a building and prediction accuracy of regression equation estimated with over the long term earthquake observation, 13^{th} JEES, 2010, pp.1530-1537 (in Japanese) .
7) Toshihide Kashima: Strong motion records observed in BRI buildings during the 2011 off the Pacific coast of Tohoku Earthquake, Summaries of Technical Papers of 2011 AIJ Annual Meeting, Structure II, 2011, pp. 319-320 (in Japanese).
8) Yoshihiro Ogata, Kiyoshi Hirotani, Naoyuki Aizawa, Norio Inoue, Takashi Nozawa: A study of initial stiffness on the building changed by passing age at small and medium-sized earthquake ground motion by ARX model, Summaries of Technical Papers of 2011 AIJ Annual Meeting, Structure II, 2011, pp. 983-984 (in Japanese).
9) Shiga, Toshio, Akenori Shibata, Jun'ichi Shibuya, and Jun'ichi Takahashi: Observations of strong earthquake motions and nonlinear response analyses of the building of architectural and civil engineering departments, Tohoku University, Transactions of Architectural Institute of Japan, No.301, 1981, pp.119-130 (in Japanese with English abstract).
10) Tanaka, Shoko and Masato Motosaka: Natural period change of an existing building during the 2008 Iwate-Miyagi Nairiku Earthquake, 2008,pp.126-127, JAEE Annual Meeting (in Japanese).
11) Masato Motosaka, Makoto Homma, Serdar Kuyuk H., and Francisco Arrecis: Development of an Integrated Early Warning and Structural Monitoring System to Real Time Earthquake Information. Architectural Institute of Japan Technology Report No.14, Vol.28, Oct. 2008, pp. 669-674 (in Japanese with English abstract).
12) Tsamba, Tsoggerel, and Masato Motosaka: Investigation of dynamic behavior of a damaged 9-story building during the 2011 off the Pacific Coast Tohoku Earthquake, 2011-JAEE Annual Meeting, 2011, pp. 44-45.
13) Takahashi, Yoshiyuki, Kazuya Mitsuji, and Masato Motosaka: Estimation of vibration characteristics of the existing building by using Kalman Filter, Tohoku Journal of Natural Disaster Science, No.45, 2010, pp.107-111 (in Japanese).
14) Motosaka, Masato and Masayuki Nagano: "Dynamic partial uplift analysis of a structure on a 3-D layered half space based on recursive evaluation of Interaction forces using dynamic stiffness of the unbounded soil in frequency domain, Journal of Structural and Construction Engineering, AIJ, No.45, 1993, pp.79-88 (in Japanese with English abstract).
15) Anthony Teolis: Computational signal processing with wavelets, 1998

(Original Japanese Paper Published: November, 2012)
(English Version Submitted: October 10, 2014)
(English Version Accepted: November 2, 2014)